Estimations of Gross Primary Production and Evapotranspiration over the Terrestrial Ecosystems in China

Article · December 2011

CITATIONS
10

READS
339

4 authors, including:

Xinglan Li
Beijing Normal University
66 PUBLICATIONS **1,779** CITATIONS
SEE PROFILE

Wenping Yuan
Beijing Normal University
276 PUBLICATIONS **14,663** CITATIONS
SEE PROFILE

Xiao Cheng
Sun Yat-Sen University
224 PUBLICATIONS **4,528** CITATIONS
SEE PROFILE

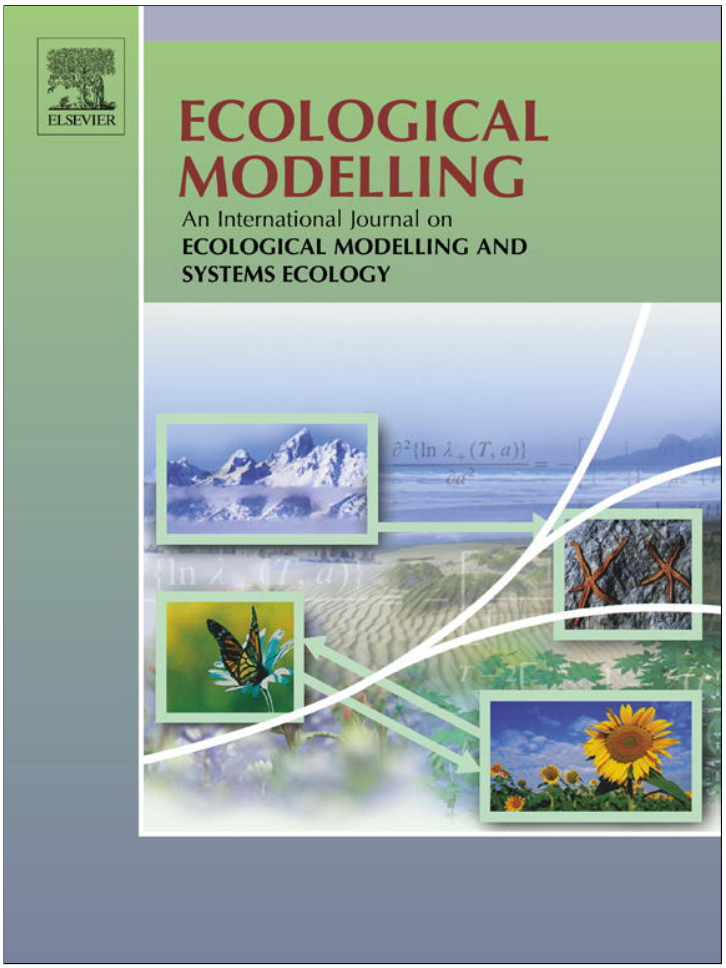

Ecological Modelling 261–262 (2013) 80–92

Contents lists available at SciVerse ScienceDirect

Ecological Modelling

journal homepage: www.elsevier.com/locate/ecolmodel

Estimation of gross primary production over the terrestrial ecosystems in China

Xianglan Li[a,b], Shunlin Liang[a,b,c,*], Guirui Yu[d], Wenping Yuan[a,b,*], Xiao Cheng[a,b], Jiangzhou Xia[a,b], Tianbao Zhao[e], Jinming Feng[b,e], Zhuguo Ma[e], Mingguo Ma[f], Shaomin Liu[g], Jiquan Chen[h,i], Changliang Shao[j], Shenggong Li[k], Xudong Zhang[l], Zhiqiang Zhang[m], Shiping Chen[j], Takeshi Ohta[n], Andrej Varlagin[o], Akira Miyata[p], Kentaro Takagi[q], Nobuko Saiqusa[r], Tomomichi Kato[s]

[a] State Key Laboratory of Remote Sensing Science, Jointly Sponsored by Beijing Normal University and Institute of Remote Sensing Applications of Chinese Academy of Sciences, Beijing 100875, China
[b] College of Global Change and Earth System Science, Beijing Normal University, Beijing 100875, China
[c] Department of Geography, University of Maryland, College Park, MD 20742, USA
[d] Key Laboratory of Ecosystem Network Observation and Modeling, Synthesis Research Center of Chinese Ecosystem Research Network, Institute of Geographic Sciences and Natural Resources Research, Chinese Academy of Sciences, Beijing 100101, China
[e] Key Laboratory of Regional Climate-Environment Research for the Temperate East Asia, Institute of Atmospheric Physics, Chinese Academy of Sciences, Beijing 100029, China
[f] Cold and Arid Regions Environmental and Engineering Research Institute, Chinese Academy of Sciences, Lanzhou, Gansu 730000, China
[g] Sate Key Laboratory of Remote Sensing Science, School of Geography, Beijing Normal University, Beijing 100875, China
[h] International Center for Ecology, Meteorology and Environment (IceMe), Nanjing University of Information Science and Technology, Nanjing 210044, China
[i] Landscape Ecology and Ecosystem Science, Department of Environmental Sciences, University of Toledo, Toledo, OH 43606, USA
[j] State Key Laboratory of Vegetation and Environmental Change, Institute of Botany, Chinese Academy of Sciences, Beijing 100093, China
[k] Institute of Geographic Sciences and Natural Resources Research, Chinese Academy of Sciences, Beijing 100101, China
[l] Institute of Forestry Research, Chinese Academy of Forestry, Beijing 100091, China
[m] College of Soil & Water Conservation, Beijing Forestry University, Beijing 100083, China
[n] Graduate School of Bioagricultural Sciences, Nagoya University, Faro-Cho, Chikusa-Ku, Nagoya 464-8601, Japan
[o] A.N. Severtsov Institute of Ecology and Evolution, Russian Academy of Sciences, Lenisky pr., 33, Moscow 119071, Russia
[p] National Institute for Agro-Environmental Sciences, Tsukuba 305-8604, Japan
[q] Teshio Experimental Forest, Field Science Center for Northern Biosphere, Hokkaido University, Toikanbetsu, Horonobe, Teshio 098-2943, Japan
[r] Center for Global Environmental Research, National Institute for Environmental Studies, Onogawa 16-2, Tsukuba, Ibaraki 305-8506, Japan
[s] National Institute for Environmental Studies, Tsukuba, Ibaraki 305-8569, Japan

ARTICLE INFO

Article history:
Received 27 June 2012
Received in revised form 31 January 2013
Accepted 18 March 2013

Keywords:
EC-LUE model
Gross primary production
Eddy covariance
MODIS
MERRA

ABSTRACT

Gross primary production (GPP) is of significant importance for the terrestrial carbon budget and climate change, but large uncertainties in the regional estimation of GPP still remain over the terrestrial ecosystems in China. Eddy covariance (EC) flux towers measure continuous ecosystem-level exchange of carbon dioxide (CO_2) and provide a promising way to estimate GPP. We used the measurements from 32 EC sites to examine the performance of a light use efficiency model (i.e., EC-LUE) at various ecosystem types, including 23 sites in China and 9 sites in adjacent areas with the similar climate environments. No significant systematic error was found in the EC-LUE model predictions, which explained 79% and 62% of the GPP variation at the validation sites with C_3 and C_4 vegetation, respectively. Regional patterns of GPP at a spatial resolution of 10 km × 10 km from 2000 to 2009 were determined using the MERRA (Modern Era Retrospective-analysis for Research and Applications) reanalysis dataset and MODIS (MODerate resolution Imaging Spectroradiometer). China's terrestrial GPP decreased from southeast toward the northwest, with the highest values occurring over tropical forests areas, and the lowest values in dry regions. The annual GPP of land in China varied between 5.63 Pg C and 6.39 Pg C, with a mean value of 6.04 Pg C, which accounted for 4.90–6.29% of the world's total terrestrial GPP. The GPP densities of most vegetation types in China such as evergreen needleleaf forests, deciduous needleleaf forests, mixed forests, woody savannas, and permanent wetlands were much higher than the respective global GPP

* Corresponding authors at: State Key Laboratory of Remote Sensing Science, Jointly Sponsored by Beijing Normal University and Institute of Remote Sensing Applications of Chinese Academy of Sciences, Beijing 100875, China.
E-mail addresses: sliang@umd.edu (S. Liang), wenpingyuancn@yahoo.com (W. Yuan).

0304-3800/$ – see front matter Published by Elsevier B.V.
http://dx.doi.org/10.1016/j.ecolmodel.2013.03.024

densities. However, a high proportion of sparsely vegetated area in China resulted in the overall low GPP. The inter-annual variability in GPP was significantly influenced by air temperature ($R^2 = 0.66$, $P < 0.05$), precipitation ($R^2 = 0.71$, $P < 0.05$), and normalized difference vegetation index (NDVI) ($R^2 = 0.83$, $P < 0.05$), respectively.

Published by Elsevier B.V.

1. Introduction

Terrestrial ecosystems, driving most seasonal and inter-annual variations in atmospheric CO_2 concentration, have taken up about 20–30% of the annual total anthropogenic CO_2 emission as organic compounds over the last two and half decades (Canadell et al., 2007). Gross primary productivity (GPP), defined as the sum of photosynthetic carbon uptake by vegetation in terrestrial ecosystems, is a start of the carbon biogeochemical cycle and the principle indicator of biosphere carbon flux. Moreover, GPP contributes to human welfare because it is the basis for food, fiber and wood production, and retains human development (Beer et al., 2010). Predicting the GPP of terrestrial ecosystems has received increasing attention in global change studies (Canadell et al., 2000).

Numerous ecosystem models have been used to quantify the spatio-temporal variations in terrestrial vegetation production at large scales in China (Xiao et al., 1998; Liu et al., 1999; Chen et al., 2001; Liu, 2001; Piao et al., 2001; Gong et al., 2002; Tao et al., 2003). However, different ecosystem models are inconclusive regarding the magnitude and spatial distribution of GPP at the regional scales. Chen et al. (2001) quantified annual GPP in China as 12.26 Pg C, which is 3.14 times the estimate of Piao et al. (2001), who estimated China's annual primary production to be 3.90 Pg C (Table 1). Model outputs were indicated by low confidence at regional scales due to the following major limitations: (1) the spatial and temporal heterogeneity of ecosystem processes used by models, (2) the nonlinearity of the functional responses of ecosystem processes to environmental variables, (3) the requirements of both physiological and site-specific parameters, and (4) inadequate validation against observation (Baldocchi et al., 1996; Friend et al., 2007; Yuan et al., 2010).

Of all the predictive methods, the light use efficiency (LUE) model may have the most potential to adequately address the spatial and temporal dynamics of GPP because it is practical and has a theoretical basis (Running et al., 2000, 2004). The light use efficiency model is based on process-based algorithms that emphasize the uniqueness, similarity, and consistency of ecosystem processes in both time and space and it, therefore, avoids the problem of responsive nonlinearity of ecosystem processes to environmental variables (Yuan et al., 2010). Moreover, the light use efficiency model integrates remote sensing observations to provide consistent model inputs in time and space.

EC-LUE (Eddy Covariance Light Use Efficiency) was developed to simulate daily GPP, driven by four variables including the normalized difference vegetation index (NDVI), photosynthetically active radiation (PAR), air temperature and the evaporative fraction (the ratio of latent heat to the sum of latent and sensible heat) (Yuan et al., 2007, 2010). The EC-LUE model is an alternative approach that enables mapping of daily GPP over large areas because the potential LUE is invariant across various land cover types, and all driving forces of the model can be derived from remote sensing data or existing climate observation networks. The EC-LUE model was calibrated and validated using estimated GPP from eddy covariance towers in the AmeriFlux and EuroFlux networks covering a variety of forests, grasslands, and savannas (Yuan et al., 2007, 2010). However, EC-LUE has not been validated over the China ecosystem due to limited EC measurements. This study had the following objectives: (1) to examine the performance of the EC-LUE model over the terrestrial ecosystems in China, (2) to quantify the spatial and temporal patterns of GPP over the land in China, and (3) to investigate the inter-annual variability of GPP and environmental regulations during the period 2000–2009.

Table 1
Estimation of GPP in different terrestrial models.

Model	GPP (Pg C yr^{-1})	Study period	References
TEM	7.31	1993–1996	Xiao et al. (1998)
CASA	3.90	1997	Piao et al. (2001)
RSM	12.26	1990	Chen et al. (2001)
CEVSA	6.18	1981–1998	Tao et al. (2003)
BEPS	4.42	2001	Feng et al. (2007)
TEPC	9.44	2001	Liu (2001)
Revised CASA	6.24	1989–1993	Zhu et al. (2007)
EC-LUE	6.04	2000–2009	In this study

Abbreviations: TEM: terrestrial ecosystem model, CASA: Carnegie–Ames–Stanford-approach, CEVSA: carbon exchange between vegetation, soil, and the atmosphere, BEPS: boreal ecosystem productivity simulator, TEPC: terrestrial ecosystem production process model in China, EC-LUE: Eddy covariance and light use efficiency, and RSM: remote sensing model.
When GPP values are not available in some references, GPP was calculated by NPP multiplying a factor of 2.

2. Materials and methods

2.1. The EC-LUE model

In this study, we used the EC-LUE (Eddy Covariance – Light Use Efficiency) model to estimate GPP over the terrestrial ecosystem in China. The EC-LUE model was developed, parameterized, and validated using estimated GPP based on eddy covariance measurements covering various ecosystem types. Previous EC-LUE models were hampered by poor simulation of the evaporative fraction at large spatial scales, which was used to present the moisture constraint on light use efficiency. Net radiation (R_n) is substituted for both the latent heat (LE) flux and sensible heat (H) flux (Yuan et al., 2010), thus omitting the soil heat flux. R_n can be derived from existing climate observation networks. The revised RS-PM (Remote Sensing-Penman Monteith) model was used to estimate evapotranspiration (ET), which is equivalent to LE (Yuan et al., 2010). The calibrated values for optimal temperature and potential light use efficiency of the EC-LUE model were 21 °C and 2.25 g C MJ^{-1}, respectively (Yuan et al., 2010).

In the latest study, the EC-LUE and the revised RS-PM models were calibrated and validated using estimated GPP based on EC measurements at twenty-two and thirty-three sites from the AmeriFLUX and EuroFLUX networks, respectively (Yuan et al., 2010). The revised RS-PM model explained 82% and 68% of the observed variations of ET for all the calibration and validation sites, respectively. Using estimated ET as the input, the EC-LUE model explained 75% and 61% of the observed GPP variation for calibration and validation sites, respectively. Global patterns of GPP at a spatial resolution of 10 km × 10 km from 2000 to 2003 were determined using the EC-LUE model based on the global MERRA and MODIS datasets. The global GPP estimates of 110 ± 21 Pg C yr^{-1} agreed well with other global models from the literature (Beer et al., 2010). Because the potential LUE of the EC-LUE model is invariant across

various land cover types, it is easy to map daily GPP over large areas.

2.2. Data at EC site

Twenty-three EC sites in China, covering various ecosystem types such as forests, grasslands, croplands, and prairies, were included in this study to validate the EC-LUE model (Table 2). To substantially validate the EC-LUE model over different ecosystem types, we also used the measurements of 9 EC sites in several Asian countries including Russia, Korea, and Japan since similar climate conditions occurred in both China and these other Asian regions. For example, site information of TKY was described in previous reports (Saigusa et al., 2005). Half-hourly or hourly averaged regional radiation (Ra), photosynthetically active radiation (PAR), air temperature (Ta), and friction velocity (u^*) were used with the net ecosystem exchange of CO_2 (NEE) in this study.

Data analyses procedures were presented in Yuan et al. (2010). Briefly, daily NEE, ecosystem respiration (Re), and meteorological variables were synthesized based on half-hourly or hourly values. The tower-based GPP was calculated as the result of NEE and Re. Daytime respiration Re is usually developed from nighttime NEE measurements which equals to night respiration, and estimated by using daytime temperature and a linear equation describe the temperature dependence of respiration. Desai et al. (2008) applied 23 different methods to 10 site years of EC in order to investigate the effects of partitioning method choice, data gaps, and inter-site variability on estimated GPP and Re, which indicated that most methods differed by less than 10% in estimates of both GPP and Re. This confirms that the uncertainty of site-based GPP calculation may not enlarge the difference between predicted and observed GPP. The daily values were indicated as missing when missing data was more than 20% of the entire data on a given day. Otherwise, daily values were calculated by multiplying the averaged hourly rate by 24 h.

The normalized difference vegetation index (NDVI) and the leaf area index (LAI) for the EC sites were determined from Moderate Resolution Imaging Spectroradiometer (MODIS) data. MODIS ASCII subset data used in this study were generated from MODIS Collection 5 data that was downloaded directly from the Oak Ridge National Laboratory Distributed Active Center (ORNL DAAC) website. The 8-day MODIS LAI (MOD15A2) and 16-day MODIS NDVI (MOD13A2) data at 1 km × 1 km spatial resolution were the basis for model verification in the EC flux sites. Only the NDVI and LAI values of the pixel containing the tower were used. Quality control (QC) flags, which signal cloud contaminate in each pixel, were examined to screen and reject poor quality NDVI and LAI data.

2.3. Data at regional scale

For regional estimates of GPP, we used input datasets for air temperature (T) and relative humidity (Rh) obtained from 753 stations in China by meteorological interpolation and net radiation (R_n) and photosynthetically active radiation (PAR) from the MERRA (Modern Era Retrospective Analysis for Research and Applications) archive from 2000 to 2009 (Global Modeling and Assimilation Office, 2004). MERRA is a NASA reanalysis for the satellite era data using the Goddard Earth Observing System Data Assimilation System Version 5 (GEOS-5). MERRA uses data from all available global surface weather observations every 3 h. GEOS-5 was used to interpolate and grid the MERRA point data over a short time sequence, and it produces an estimate of climatic conditions for the world at 10 m above the land surface (approximating canopy height conditions) and at a resolution of 10 km × 10 km. The MERRA reanalysis dataset has been validated carefully at the global scale using surface meteorological data sets to evaluate the uncertainty of various meteorological factors (i.e., temperature, radiation, humidity, and energy balance). The reanalysis showed that MERRA considerably reduced the energy and water imbalance. Detailed information on the MERRA dataset is available at the website http://gmao.gsfc.nasa.gov/research/merra.

Global 8-day MODIS LAI (MOD15A2) and 16-day MODIS NDVI (MOD13A2) data were used in this study. Quality control (QC) flags were examined to screen and reject poor quality NDVI and LAI data. We temporally filled in the missing or unreliable LAI and NDVI at each 1-km MODIS pixel based on their corresponding quality assessment data fields as proposed by Zhao et al. (2005). If the first (or last) 8-day LAI (16-day NDVI) data were unreliable or missing, they were replaced by the closest reliable 8-day (or 16-day) values. Both spatially related average and total GPP over the terrestrial ecosystems in China are area-weighted.

Meanwhile, GPP densities among various vegetation types in China were compared with those values in global terrestrial ecosystems. We also compared the difference between GPP estimated by the EC-LUE model and MODIS product in China. The annual MODIS GPP during the period from 2000 to 2010 was downloaded from the websites as following: http://http.ntsg.umt.edu/pub/MODIS/Mirror/MOD17_Science_2010/MOD17A3/Geotiff/.

2.4. Statistical analysis

The following three metrics were used to evaluate the performance of the EC-LUE model:

(1) The coefficient of determination (R^2), which represents the amount of variation in the observation that was explained by the models.
(2) Predictive error (PE), which quantifies the difference between simulated and observed values:

$$PE = \overline{S} - \overline{O} \quad (1)$$

where $\overline{S}$ and $\overline{O}$ are mean simulated and mean observed values, respectively.

(3) Relative predictive error (RPE) computed as:

$$RPE = \frac{\overline{S} - \overline{O}}{\overline{O}} \times 100\% \quad (2)$$

Moreover, we used the standard deviation (SD) of the annual GPP to characterize the absolute inter-annual variability (AIAV) and used the coefficient of variation (CV, the ratio of SD and mean value of annual GPP) to characterize the relative inter-annual variability (RIAV).

3. Results and discussion

3.1. Model performance

Over various ecosystem types such as forests, croplands, and grasslands, the EC-LUE model successfully predicted the magnitudes and seasonal variations of GPP derived by the observed environmental variables (i.e., T, PAR, and R_n) (Fig. 1). The predicted GPP and estimated GPP from the EC measurement time series at the validation sites demonstrated distinct seasonal cycles and matched well. At most sites, GPP values were near zero in the winter because low temperature and frozen soil inhibited photosynthetic activities.

Collectively, the EC-LUE model explained about 79% of the variation of the 8-day GPP estimated at validation sites dominated by

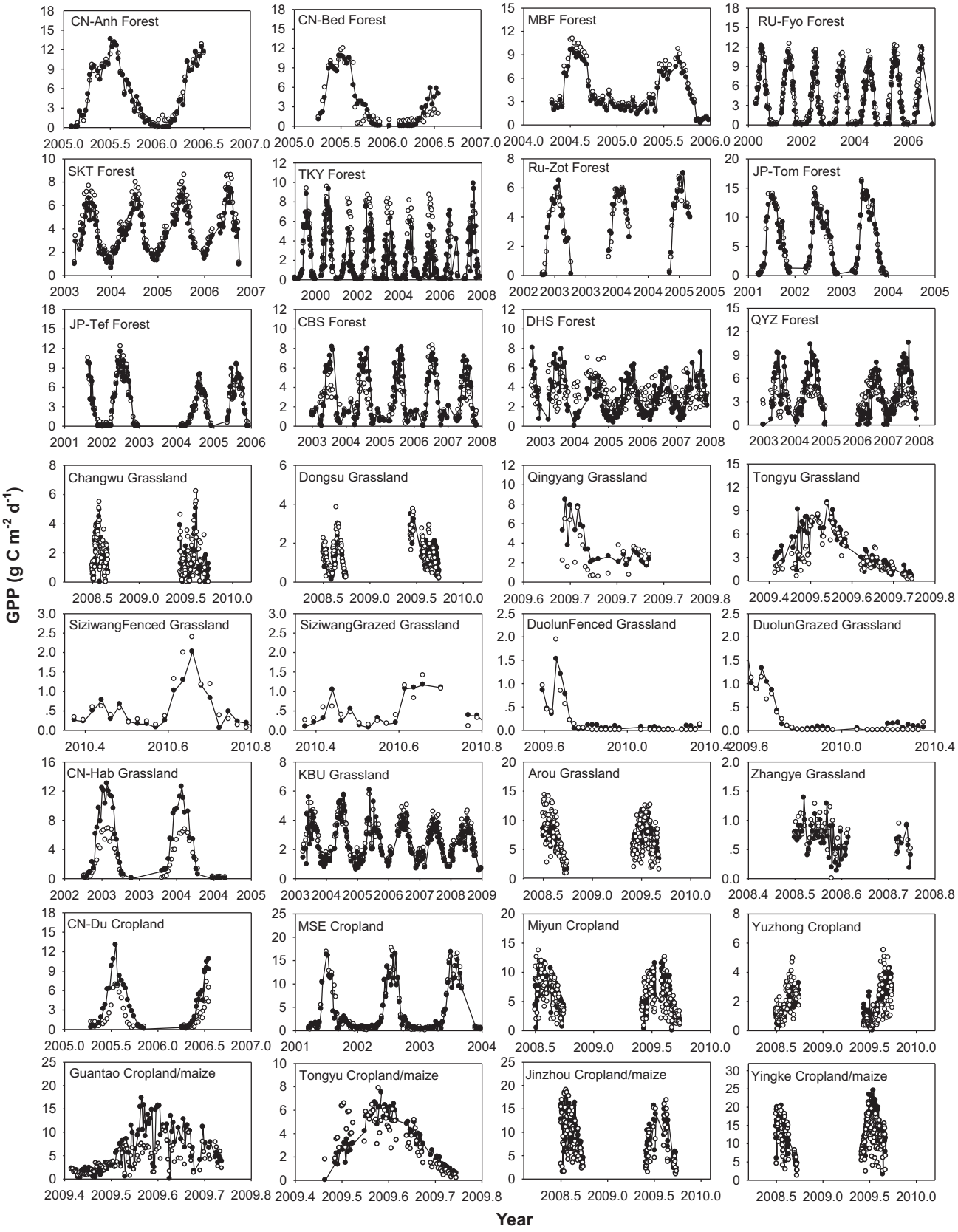

Fig. 1. Variation in the 8-day mean value of predicted and observed GPP at the EC-LUE model validation sites in China. The black solid lines represent the predicted GPP, and the open circle dots represent observed GPP.

Table 2
Name, location, vegetation type and available years of the study sites used for the EC-LUE model validation.

Site name	Latitude, longitude	Vegetation type	Available years
CN-Du	42.05°N, 116.67°W	Cropland	2005–2006
Miyun	40.63°N, 117.32°W	Cropland	2008–2009
MSE	36.05°N, 140.03°W	Cropland	2001–2004
Yuzhong	35.95°N, 104.13°W	Cropland	2008–2009
Guantao	36.52°N, 105.13°W	Cropland/Maize	2009
Jinzhou	41.18°N, 121.21°W	Cropland/Maize	2008–2009
TongyuCrop	44.57°N, 122.88°W	Cropland/Maize	2009
Yingke	38.86°N, 100.41°W	Cropland/Maize	2008–2009
CBS	42.40°N, 127.09°W	Forest	2003–2008
CN-Anh	30.48°N, 116.98°W	Forest	2005–2006
CN-Bed	39.53°N, 116.25°W	Forest	2005–2006
DHS	23.17°N, 112.53°W	Forest	2002–2008
JP-Tef	45.06°N, 142.11°W	Forest	2002–2006
JP-Tom	42.74°N, 141.52°W	Forest	2001–2004
MBF	44.38°N, 142.32°W	Forest	2004–2006
QYZ	26.74°N, 115.07°W	Forest	2002–2008
RU-Fyo	56.46°N, 32.92°W	Forest	2000–2006
RU-Zot	60.80°N, 89.35°W	Forest	2002–2005
SKT	48.35°N, 108.65°W	Forest	2003–2007
TKY	36.15°N, 137.42°W	Forest	1999–2007
Arou	38.04°N, 100.46°W	Grassland	2008–2009
Changwu	35.20°N, 107.67°W	Grassland	2008–2009
CN-HaM	37.37°N, 101.18°W	Grassland	2002–2004
Dongsu	44.09°N, 113.57°W	Grassland	2008–2009
DuolunFenced	42.04°N, 116.29°W	Grassland	2009–2010
DuolunGrazed	42.05°N, 116.28°W	Grassland	2009–2010
KBU	47.21°N, 108.74°W	Grassland	2003–2009
Qingyang	35.59°N, 107.54°W	Grassland	2009
SiziwangFenced	41.23°N, 111.57°W	Grassland	2010
SiziwangGrazed	41.28°N, 111.68°W	Grassland	2010
TongyuGrass	44.57°N, 122.88°W	Grassland	2008–2009
Zhangye	39.09°N, 100.30°W	Grassland	2008

C_3 plants and 62% by C_4 vegetations (Fig. 2), respectively. Individually, the coefficients of determination (R^2) between observed GPP and predicted GPP varied from 0.48 to 0.98, but all of them were statistically significant at $P < 0.05$ (Fig. 3). For the R^2 values between observed and estimated ET, similar tendency was found with a range from 0.39 at. and 0.97 (Fig. 3). The EC-LUE model explained significant amounts of GPP variability at the individual sites; however, large differences between the predicted and the estimated GPP values from EC measurements existed at a few sites. For example, the model underestimated GPP at Guantao, Jinzhou, Tycropland, and Yingke, with the relative predictive errors being −55%, −43%, −35%, and −40%, respectively. At the other EC sites, the EC-LUE model gave a good prediction with RPE values less than 25% (Fig. 3). In general, ET model showed better performance than GPP model in terms of RMSE (Fig. 3).

Several aspects including plant species, satellite data, meteorology data, ET simulation, and EC site data, should be considered when evaluating the EC-LUE model performance. The discrepancies between predicted and estimated GPP from EC measurement values occurred mainly in maize croplands such as Guantao, Tycropland, Jinzhou, and Yingke. Under the same climate conditions, C_4 crops have a greater photosynthetic capacity and more rapid accumulation of green leaf area than C_3 crops (Chapin et al., 2002; Turner et al., 2003; Suyker et al., 2005; Zhang et al., 2008). The major cause for the underestimation of GPP at the maize croplands was because parameters of the EC-LUE model were calibrated

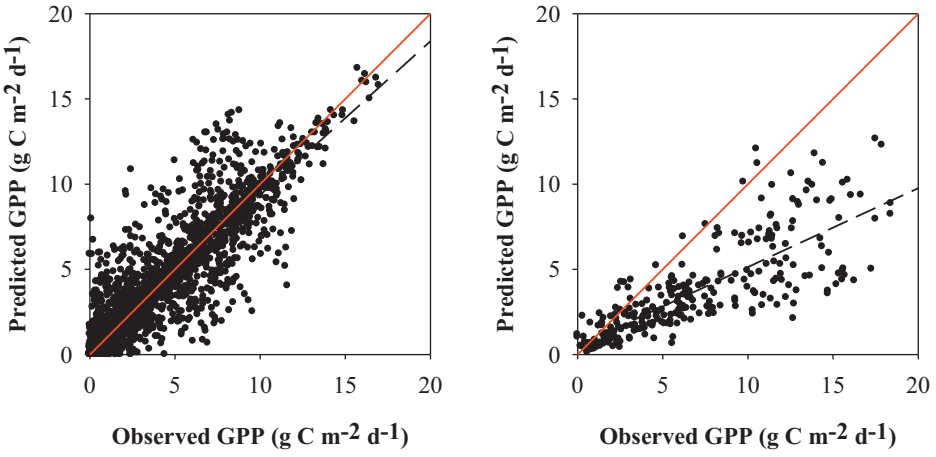

Fig. 2. Comparison of GPP observations from the flux tower sites and predictions by the EC-LUE model from C_3 vegetation (a) and C_4 vegetation (b) types, respectively. The EC-LUE model could explain 79% and 62% of GPP variations for C_3 ($y = 0.90x + 0.34$, $R^2 = 0.79$, $P < 0.05$) and C_4 vegetation types ($y = 0.46x + 0.50$, $R^2 = 0.62$, $P < 0.05$), respectively.

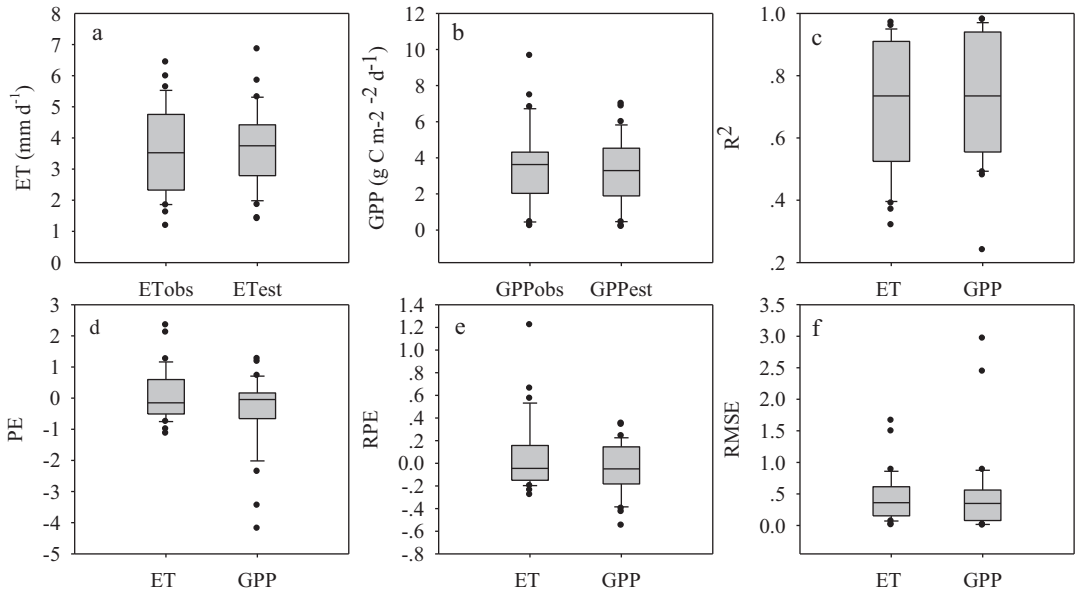

Fig. 3. Statistic analysis of the daily ET and GPP that observed at the 32 EC sites and predicted by the respective RS-PM and EC-LUE models. (a) Average daily ET compared between the observed and the predicted values, (b) average daily GPP compared between the observed and the predicted values, (c) coefficient of determination (R^2), (d) Predicted error (PE), (e) Relative predicted error (RPE), (f) Root mean square error (RMSE). Plots showed the median, upper and lower quartile, minimum and maximum outliers (points) at the 32 EC sites.

in C_3 plant dominant ecosystems. The underestimation of GPP for maize was close at the four croplands, and the peak of the simulated GPP was 50% smaller than the observed GPP, which is similar to the previous result (Yuan et al., 2010). Consistent potential light use efficiency was derived for C_4 crops to improve the performance of the EC-LUE model in the maize croplands. In this study, the mean 8-day GPP estimations from four maize cropland sites (Guantao, Jinzhou, Tycropland, and Yingke) were multiplied by a revision factor of 1.5 (Fig. 1), and the EC-LUE model performed better in the correlation relationship between the observed and the predicted GPP. Yuan et al. (2010) indicated that the calibrated values for optimal temperature and potential LUE were 19 °C and 4.06 g C MJ^{-1} in maize cropland sites, and the EC-LUE model successfully predicted the magnitudes and seasonal variations of observed GPP using different parameters for C_3 and C_4 crops, respectively. Therefore, the EC-LUE model could be revised by changing the parameters for the C_4 vegetation type, and it is necessary to use a spatial distribution map of C_3 and C_4 crops to improve the accuracy of quantifying GPP across large scales. There were difficulties in the revision of the EC-LUE model because there is no distribution map of C_4 crops. The harvested area of China's maize cropland only accounts for about 3.5% of the total land area (FAOSTAT, 2008), so the GPP estimate of maize croplands did not significantly affect the terrestrial GPP total.

The EC-LUE model makes it possible to map daily GPP over large areas because the potential LUE is invariant across various land cover types and all driving forces of the model can be derived from remote sensing data or existing climate observation networks. EC measurements at multiple sites over the North American and Europe have been used to calibrate and validate the EC-LUE model (Yuan et al., 2007, 2010). In this study, model validation at 36 EC sites suggested that the EC-LUE model was robust and reliable across most of the biomes and geographic regions in China. The coefficient determination (R^2) between GPP estimates and GPP observations for the 8-day results ranged from 0.79 for C_3 vegetation to 0.62 for C_4 vegetation, respectively. We did not calibrate the model parameters based on the EC measurements in China, which indicates constant model parameters at various regions.

Satellite data to provide temporally and spatially continuous information over the vegetated surface significantly strengthened model performances across the regional scales. This study used MODIS/Terra NDVI and LAI products that were downloaded directly from the MODIS Web site. Because no attempt was made to improve the quality of the NDVI or LAI data, any noise or error in the satellite data would be transferred to GPP simulations. Additionally, the accuracy of regional or global estimates of GPP is highly dependent on the meteorology dataset. Fig. 3 showed the performance of the EC-LUE model driven by tower-specific meteorology and by the global MERRA meteorology dataset, respectively. The model driven by tower-specific meteorology data explained 91% of the variations of the annual mean GPP across the validation sites (Fig. 4a) and provided no systematic errors in model predictions. In contrast, using the MERRA dataset significantly decreased the model performance and explained 85% of the variations of GPP (Fig. 4b). The accuracy of the existing meteorological reanalysis data sets showed marked spatial and temporal differences, which is in agreement with the previous study (Zhao et al., 2006).

In general, MERRA can denote the variability of air temperature, relative humidity and photosynthetically active radiation very well with R^2 values between EC sites and MERRA of 0.88, 0.83, and 0.76, respectively (Fig. 5). The tendency for MERRA to underestimate net surface (R_n) radiation ($R^2 = 0.61$) resulted in the lower predicted GPP (Figs. 4b and 5). Our results revealed that the biases in meteorological reanalysis can introduce substantial errors into GPP estimation and also emphasizes the necessity to minimize these biases to improve the quality of the GPP product.

Estimated ET by the revised RS-PM model was used to simulate GPP. Any simulation errors of ET will be transferred to GPP estimations. In general, the revised RS-PM model successfully predicted the variations of ET at 32 EC sites (Fig. 3). Large errors still existed at a few sites such as Changwu, SKT, and Yingke that had RPE values of 32%, 44% and −28%, respectively. The errors resulted in an overestimate and an underestimate of terrestrial GPP. There was a significant relationship between predictive errors of ET and GPP (data not shown). The simulated GPP depended greatly on the quality of the ET result, and the improved RS-PM model for ET estimate will strengthen the accuracy of the GPP estimate.

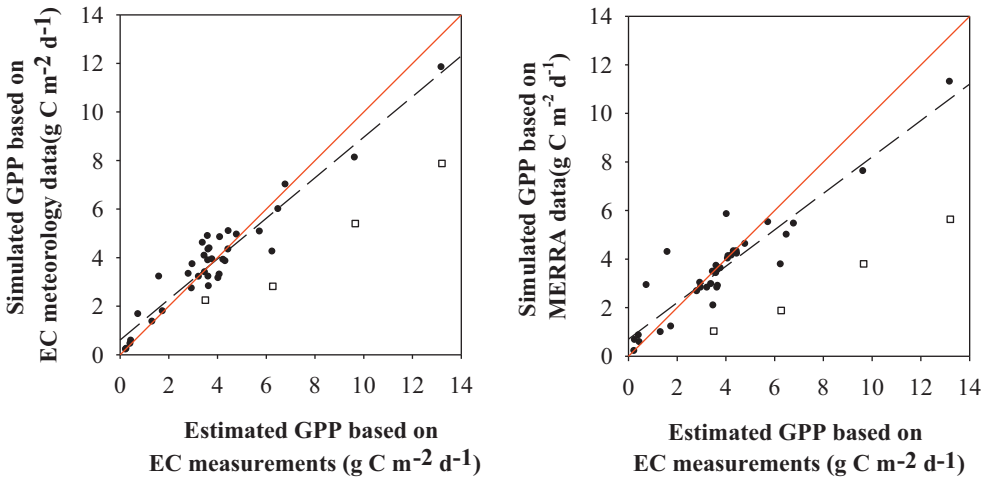

Fig. 4. Comparisons of mean GPP observations from 2000 to 2009 at each flux tower sites and the GPP estimates made by the revised EC-LUE model. These data were created using (a) tower-specific meteorology ($y = 0.84x + 0.61$, $R^2 = 0.91$) and (b) the regional MERRA meteorology ($y = 0.75x + 0.70$, $R^2 = 0.85$). The mean GPP estimations from four maize croplands (Guantao, Jinzhou, Tongyu, and Yingke) for the regression relationship were multiplied by a revision factor of 1.5. The original predicted GPP from maize croplands was indicated as open circles in each figure.

Moreover, many studies have shown that the uncertainty of model parameters was the large contributor to the overall model uncertainty (Verbeeck et al., 2006). Therefore, the assessment of the uncertainty surrounding estimates of GPP provides extremely useful information for understanding ecosystem carbon cycle and investigations on impacts of climate change. In this study, we used fixed model parameter values, however numerous of studies have showed the inversed model parameters varied within parameter range (Alton, 2011). So, it is necessary to evaluate uncertainty of GPP estimations derived from model parameters in the near future.

3.2. Spatial patterns of GPP

China's terrestrial GPP varied between 5.63 Pg C yr^{-1} and 6.39 Pg C yr^{-1} from 2000 to 2009, with a mean value of 6.04 Pg C yr^{-1}. Compared with the previous results, China's terrestrial GPP accounted for 4.90–6.29% of the world's terrestrial

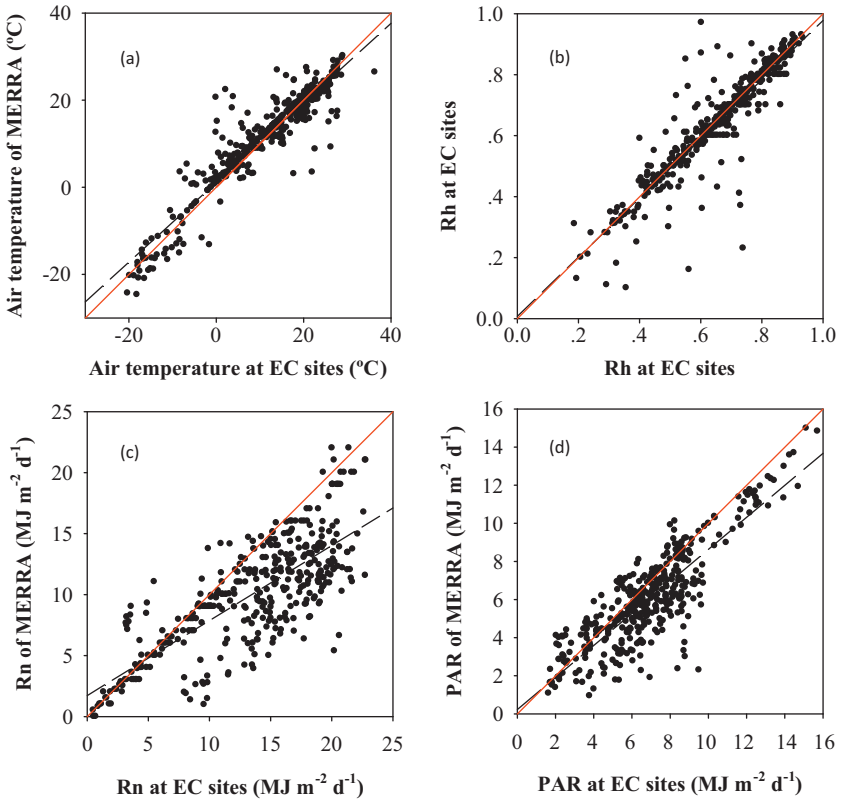

Fig. 5. Comparison of monthly average meteorology factors measured at EC sites and derived from the MERRA dataset: (a) air temperature ($y = 0.91x + 1.1$, $R^2 = 0.88$), (b) relative humidity (Rh, $y = 0.62x + 1.72$, $R^2 = 0.61$), (c) net radiation (Rn, $y = 0.97x + 0.01$, $R^2 = 0.83$), and (d) photosynthetically active radiation (PAR, $y = 0.84x + 0.22$, $R^2 = 0.76$).

total (Beer et al., 2010; Yuan et al., 2010). We calculated the MODIS GPP in China area, with a result of 5.47 Pg C yr^{-1} during the period of 2000–2009 (Table 4). It indicated that the EC-LUE model overestimated GPP by 10% when compared with MODIS GPP, especially in Xizang, Qinghai, and Xinjiang provinces. No significant difference of GPP estimation was found between EC-LUE prediction and MODIS product in other provinces (Table 3).

In this study, GPP predicted by the EC-LUE model was also comparable to other previous estimations in China (Table 1). For example, a regional estimation of GPP by Tao et al. (2003) showed 6.18 Pg C yr^{-1} using a process-based ecosystem model (i.e., the CEVAS model). Also, a comparable gross carbon uptake between 6.91 Pg C yr^{-1} and 7.33 Pg C yr^{-1} also occurred for the conterminous U.S. (Xiao et al., 2010). However, different ecosystem models are inconclusive regarding the magnitude and spatial distribution of the GPP at regional and global scales (Cao and Fian, 1998; Chen et al., 2006; Landsberg and Waring, 1997; Mu et al., 2007; Potter et al., 1993; Running et al., 1999; Xiao et al., 2004), and large uncertainties of regional GPP still remain for the terrestrial ecosystems in China. For example, a high terrestrial vegetation production of 12.26 Pg C yr^{-1} in China was found using a remote sensing model (Chen et al., 2001), which is equivalent to 2.06 times the GPP estimation in this study. Even though the same CASA model was used, large differences existed in the estimation of GPP between the studies of Piao et al. (2001) and Zhu et al. (2007). This discrepancy may be because Piao et al. (2001) used the default parameter value of potential light use efficiency (i.e., 0.389 g C m^{-2} MJ^{-1} APAR) derived by Potter et al. (1993). Zhu et al. (2007) inversed the potential light use efficiency based on field-measured NPP at 690 sites in the individual vegetation types, and the parameters were higher than the default in the CASA model. According to our estimation, vegetation GPP over the terrestrial ecosystem is disproportionate to land area in China. The total land area in China is only about 7% of the world land area and about 56–65% of this area is hills, mountains, plateau, and arid and semiarid regions (Fang and Yoda, 1990; Piao et al., 2001). A large barren or sparsely vegetated area may lead to a low GPP estimate for the terrestrial ecosystem in China.

Fig. 6 shows the spatial distribution of average GPP predicted by EC-LUE model in this study, MODIS product, and EC-LUE model in Yuan et al. (2010). Overall, similar tendency of GPP was found in China from 2000 to 2009, with GPP decreasing from the southeast toward the northwest. Also, significantly lower GPP magnitude and obvious footprint at the course resolution was found in Yuan et al. (2010) when compared with the spatial distribution of GPP in this study. Southern Hainan Island, Southwestern Yunnan, and Southeastern Tibet, where the dominant vegetation is tropical and semitropical evergreen broadleaf forests, showed high GPP values with GPP densities exceeding 2000 g C m^{-2} yr^{-1}. The average GPP of Heng-tuan Mountains, Wuyi Mountain, and the interior part of Taiwan showed relatively high values of GPP such as 1500 g C m^{-2} yr^{-1}. From the stand point of national territory, the relatively high annual production (1436–1895 g C m^{-2}) is found in Taiwan, Hainan, Fujian, Yunnan, Guangxi, and Guangdong provinces (Table 3) where both temperature and moisture requirements are fully satisfied for photosynthesis. Temperate regions have an intermediate GPP (701–1348 g C m^{-2}). The lowest GPP (<700 g C m^{-2}) is found in both cold and arid regions such as Xinjiang, Qinghai, Xizang, Ningxia, Gansu, and Inner Mongolia, where either temperature or precipitation is a limiting factor.

Estimations of average GPP densities over different land coverage were shown in Table 4. The MODIS land coverage classification product was used to identify 16 different land cover types in China. Croplands take up an average of 1.31 Pg C yr^{-1}, account for 22% of China's terrestrial GPP and have a relatively high GPP

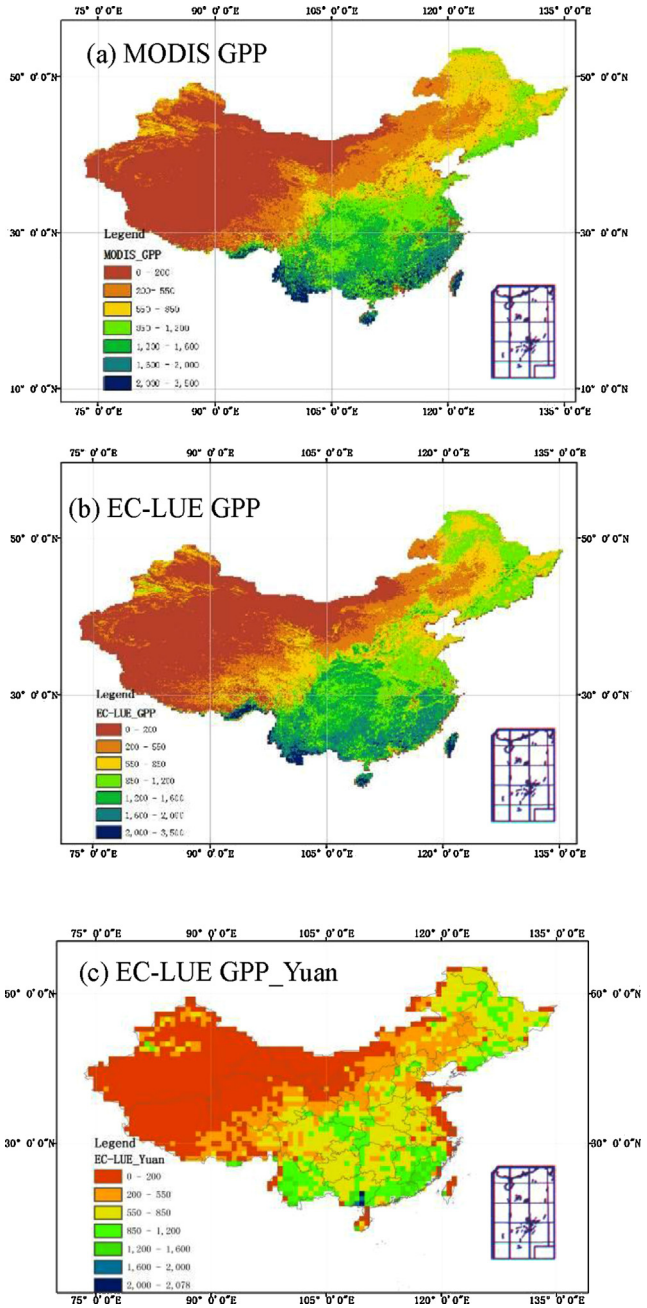

Fig. 6. Spatial distribution of the variability in GPP estimates as represented by (a) annually averaged MODIS GPP (g C m^{-2} yr^{-1}) during the period 2000–2009, (b) GPP estimation (g C m^{-2} yr^{-1}) driven by EC-LUE model with the interpolated 10 km MERRA meteorological data averaged from 2000 to 2009, (c) GPP estimation (g C m^{-2} yr^{-1}) driven by EC-LUE model with the interpolated 0.5 × 0.6 MERRA meteorological data averaged from 2000 to 2009.

density. Mixed forests that assimilate 1.19 Pg C yr^{-1} are the second most important biome in terms of the regional GPP. The third important GPP value occurred in the grasslands, and the large area of grasslands (more than twice the surface area of the mixed forests) explains their high contribution followed by woody savannas and natural vegetation mosaic. These five most productive vegetation types accounted for 81% of the total gross primary production in China. The GPP densities in barren or sparsely vegetated areas and savannas were much smaller. The averaged GPP values were relatively high over evergreen broadleaf forests, woody savannas, permanent wetlands, mixed forests and natural vegetation mosaics ranging from 1157 g C m^{-2} yr^{-1} to 1430 g C m^{-2} yr^{-1}

Table 3
Comparisons of the predicted GPP by EC-LUE model and MODIS GPP for different provinces during the period from 2000 to 2009.

Province name	EC-LUE GPP			MODIS GPP
	Area (100 km^2)	GPP density (g C m^{-2} yr^{-1})	GPP (Pg C yr^{-1})	GPP (Pg C yr^{-1})
Xinjiang	17,559	120	0.211	0.122
Qinghai	7147	255	0.182	0.085
Xizang	11,352	319	0.362	0.172
Ningxia	529	325	0.017	0.013
Gansu	4144	366	0.152	0.112
Inner Mongolia	12,925	384	0.496	0.317
Tianjin	123	588	0.007	0.005
Shanxi	1588	701	0.111	0.104
Hebei	1971	749	0.148	0.146
Shandong	1503	774	0.12	0.107
Liaoning	1547	793	0.12	0.102
Jilin	2143	793	0.17	0.164
Shanghai	48	796	0.04	0.004
Beijing	166	826	0.01	0.015
Heilongjiang	5462	835	0.46	0.402
Shaanxi	2048	909	0.19	0.174
Jiangsu	944	940	0.09	0.090
Henan	1609	981	0.16	0.140
Sichuan	4499	1007	0.45	0.416
Anhui	1331	1085	0.14	0.144
Hubei	1735	1174	0.21	0.202
Chongqing	775	1249	0.1	0.096
Hunan	1923	1310	0.25	0.265
Zhejiang	925	1327	0.12	0.141
Jiangxi	1526	1338	0.2	0.224
Guizhou	1611	1348	0.22	0.206
Guangdong	1554	1436	0.22	0.253
Guangxi	2098	1523	0.32	0.340
Yunnan	3424	1526	0.52	0.581
Fujian	1089	1548	0.17	0.210
Hainan	273	1805	0.05	0.062
Taiwan	309	1895	0.06	0.056
Sum or average	95,880	970	6.04	5.47

(Table 4). Compared with GPP densities in China, relatively high values of global GPP (974–1619 g C m^{-2} yr^{-1}) occurred in evergreen broadleaf forests, deciduous broadleaf forests, and croplands. Most of the vegetation types, such as evergreen needleleaf forests, deciduous needleleaf forests, mixed forests, woody savannas, and permanent wetlands showed regional GPP densities that were higher than global GPP by a factor of 1.74–1.98. China's GPP simulation was relatively low when compared with global GPP in a terrestrial ecosystem. This further proved that a high proportion of sparsely vegetated areas, 24% of the whole land area (Table 4), accounted for the low GPP in Chinese land.

3.3. Seasonal patterns of GPP

Our estimates showed that GPP over the terrestrial ecosystems in China exhibited strong seasonal fluctuations (Fig. 7). The seasonal patterns of GPP and its spatial variability reflected the controlling effects of the climate conditions. Because of the various climatic

Table 4
Estimations of total GPP amount and average GPP densities under different land coverage from 2000 to 2009. Global GPP density that was unpublished data was referred as a comparison.

Vegetation type	Area (100 km)	GPP (Pg C yr^{-1})	GPP density (g C m^{-2} yr^{-1})	STD (g C m^{-2} yr^{-1})	CV	Global GPP density (g C m^{-2} yr^{-1})
ENF	847	0.08	992	77	0.058	528
EBF	2472	0.35	1430	119	0.059	1619
DNF	776	0.06	829	57	0.068	460
DBF	1625	0.18	1083	55	0.052	1100
MF	9321	1.19	1273	68	0.056	731
CSH	1513	0.12	775	58	0.079	510
OSH	3487	0.09	244	19	0.068	273
WS	6020	0.83	1373	76	0.056	768
SAV	177	0.01	703	67	0.094	864
GL	23,146	0.88	382	34	0.088	402
PW	542	0.07	1332	81	0.065	672
CL	15,651	1.31	839	55	0.070	690
UBU	765	0.06	804	58	0.076	713
CRP/NVM	5848	0.68	1157	64	0.057	974
SNI	856	0.01	95	40	0.075	59
BSV	22,834	0.11	50	9	0.058	186
Sum or average	95,880	6.04	835			659

Abbreviations: evergreen needleleaf forest (ENF), evergreen broadleaf forest (EBF), deciduous needleleaf forest (DNF), deciduous broadleaf forest (DBF), mixed forest (MF), closed shrublands (CSH), open shrublands (OSH), woody savannas (WS), savannas (SAV), grasslands (GL), permanent wetlands (PW), croplands (CL), Urban and built-up (UBP), cropland/natural vegetation mosaic (CRP/NVM), snow and ice (SI), and barren or sparsely vegetated (BSV).

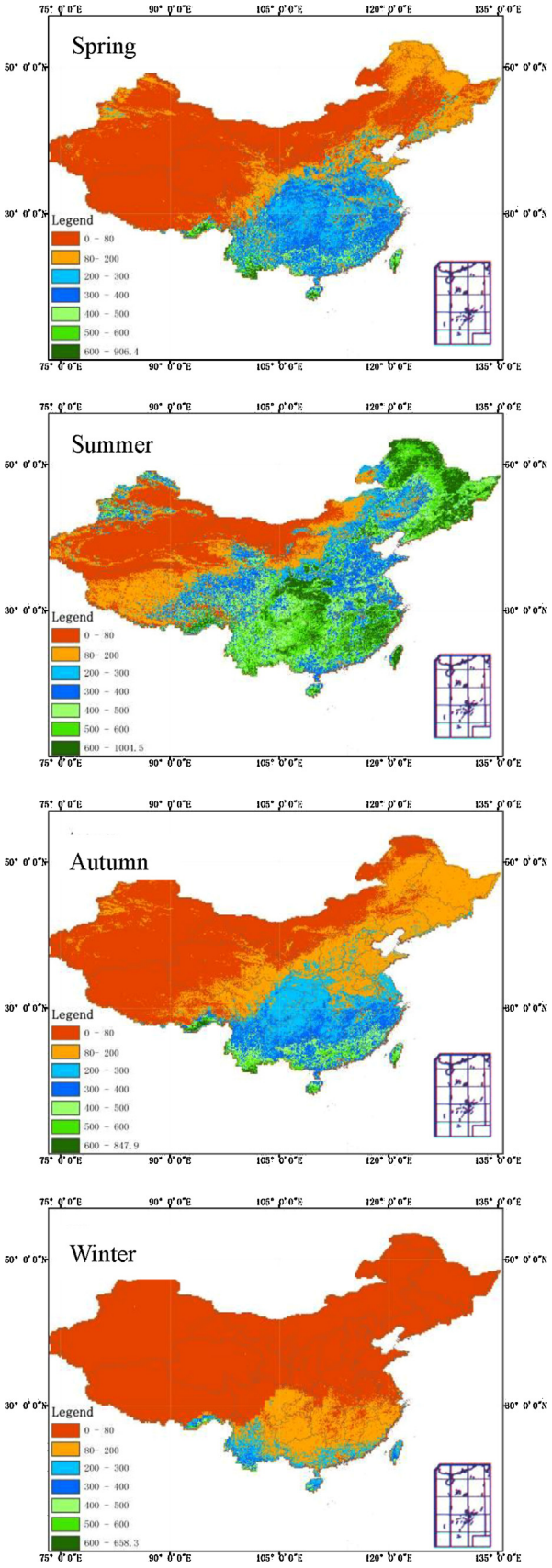

Fig. 7. Seasonal distributions of GPP (g C m^{-2}) predicted by the EC-LUE model during the period from 2000 to 2009.

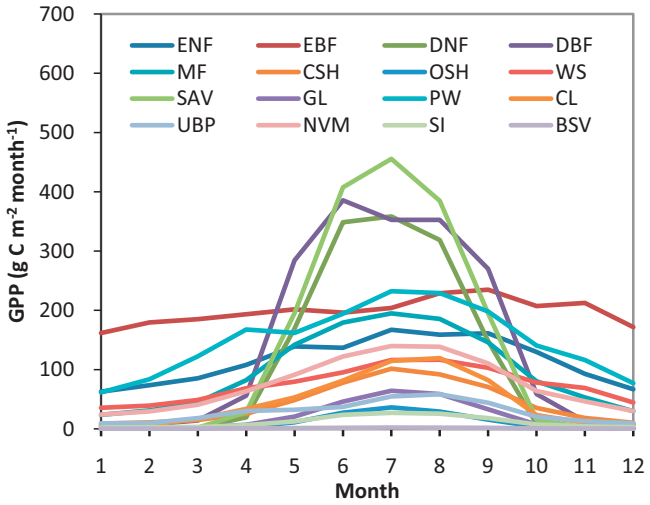

Fig. 8. Comparison between the seasonal patterns of gross primary production (GPP, g C m^{-2}) under different land use/coverage for evergreen needleleaf forest (ENF), evergreen broadleaf forest (EBF), deciduous needleleaf forest (DNF), deciduous broadleaf forest (DBF), mixed forest (MF), closed shrublands (CSH), open shrublands (OSH), woody savannas (WS), savannas (SAV), grasslands (GL), permanent wetlands (PW), croplands (CL), Urban and built-up (UBP), natural vegetation mosaic (NVM), snow and ice (SI), and barren or sparsely vegetated (BSV).

zones and vegetation distributions, the regional GPP temporal patterns varied from east to west and from north to south (Fig. 7). In the spring (March–May), the southeast significantly assimilated carbon with GPP values reaching 900 g C m^{-2} $season^{-1}$ since the growing season started in these regions. Because Taiwan and Hainan are dominated by evergreen forests, these ecosystems also assimilated carbon due to mild temperatures and moist conditions during the spring in these regions. The south of Brahmaputra areas also assimilated some carbon in the spring because of a surplus of precipitation, relatively warm temperatures and high radiation. By contrast, the barren or sparsely vegetated grassland and mixed forests, a late green up and water deficits led to a low GPP in the vast northern regions. In the summer (June–August), the middle and lower reaches of the Yangtze River regions exhibited increasing GPP values due to favorable temperature and soil moisture conditions. The vast majority of northwestern landscapes, including the Qinghai-Tibet Plateau and Inner Mongolian grasslands, exhibited much lower GPP values due to sparse vegetation and precipitation deficits. In the fall (September–November), the GPP values of the southeast regions substantially decreased relative to the GPP in the summer because vegetation began to senesce and days became shorter. The North China plain had very low GPP values less than 300 g C m^{-2} $season^{-1}$ due to crop harvesting. In the winter (December–February), the majority of China had little or no photosynthesis because the canopies of most ecosystems were dormant. The spatial patterns and magnitude of GPP in the winter were similar to those of the spring.

Fig. 8 shows the trajectories of the spatially averaged GPP for different land coverage during the period from 2000 to 2009. Deciduous needleleaf forests, deciduous broadleaf forests and savannas had the largest inter-annual variability in the spatially averaged GPP with peaks ranging from 353 g C m^{-2} $month^{-1}$ to 456 g C m^{-2} $month^{-1}$. Mixed forests, natural vegetation mosaics, croplands, and closed shrublands had relatively low GPP peaks (101–195 g C m^{-2} $month^{-1}$). Savannas and wetlands had intermediate inter-annual variability. Evergreen needleleaf forests, evergreen broadleaf forests, and permanent wetlands had the least variability. The similar trends of monthly distribution of GPP among various vegetations were found in the typical U.S. ecosystems simulated by a regression tree approach (Xiao et al., 2010). On average,

the monthly total GPP between June and August accounted for 48.8% of the annual production, whereas the monthly total GPP between November and February contributed only 13.1% in this study. Because the solar radiation is abundant and the plants thrive between June and August, maximum vegetation production occurs during this period. By contrast, low solar radiation and a minimum temperature limits plant growth from December to February. For example, the plants north of the Qinling Mountains normally stopped growing from December to February, the light use efficiency in the southern part of these mountain regions during the relative period was much lower than in summer, and the plantation growth was mainly affected by temperature resulting in low vegetation production during these three months. Hwang et al. (2008) indicated that precipitation is concentrated in the short monsoon season in East Asia, which reduces plants water availability in the dry season and decreased vegetation production. Therefore, the temporal variability of spatially averaged GPP showed a clear dependence on biome types and climate fluctuations, and both spatially averaged and integrated GPP showed inter-annual variability for each biome.

3.4. Inter-annual variability of GPP

The annual GPP varied between 5.63 Pg C yr^{-1} and 6.39 Pg C yr^{-1} over the period from 2000 to 2009, with a mean of 6.04 Pg C yr^{-1} (Fig. 8). The EC-LUE model and the MODIS GPP product estimated global GPP at 110.5 Pg C yr^{-1} (Yuan et al., 2010) and 113 Pg C yr^{-1}, respectively, and the diagnostic models estimated the global GPP to be 123 Pg C yr^{-1} (Beer et al., 2010). This study indicated that GPP in China accounted for 4.90–6.29% of the world's total terrestrial GPP. Annual GPP exhibited positive and negative anomalies for each year, where the lowest GPP was found in 2000 and then kept rising from 2000 to 2007, with a decrease in 2005. GPP values began to decrease during the period from 2007 to 2009 but were still higher than that of 2005. This tendency agreed with the inter-annual variability of MODIS GPP product and annual GPP estimation in Yuan et al. (2010) (Fig. 9). Averagely, the predicted GPP from Yuan et al. (2010) was 5.38 Pg yr^{-1} in China which was similar to MODIS GPP (5.47 Pg yr^{-1}), and 10% lower than the value in this study. In general, China's terrestrial GPP tended to increase from 2000 to 2009, which is in agreement with the seasonal and inter-annual variability of GPP at Takayama in Japan simulated by BEPS ecosystem model (Higuchi et al., 2005), a similar tendency to global vegetation production for the northern high latitudes (Zhao and Running, 2010).

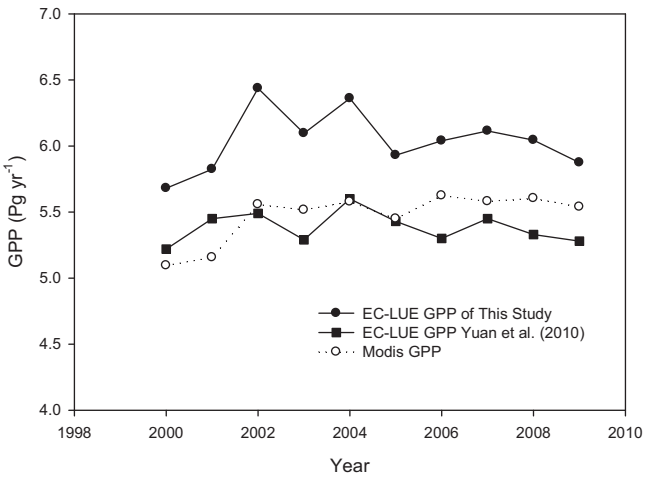

Fig. 9. Inter-annual variations of GPP of the EC-LUE model from MODIS product, Yuan et al. (2010), and this study.

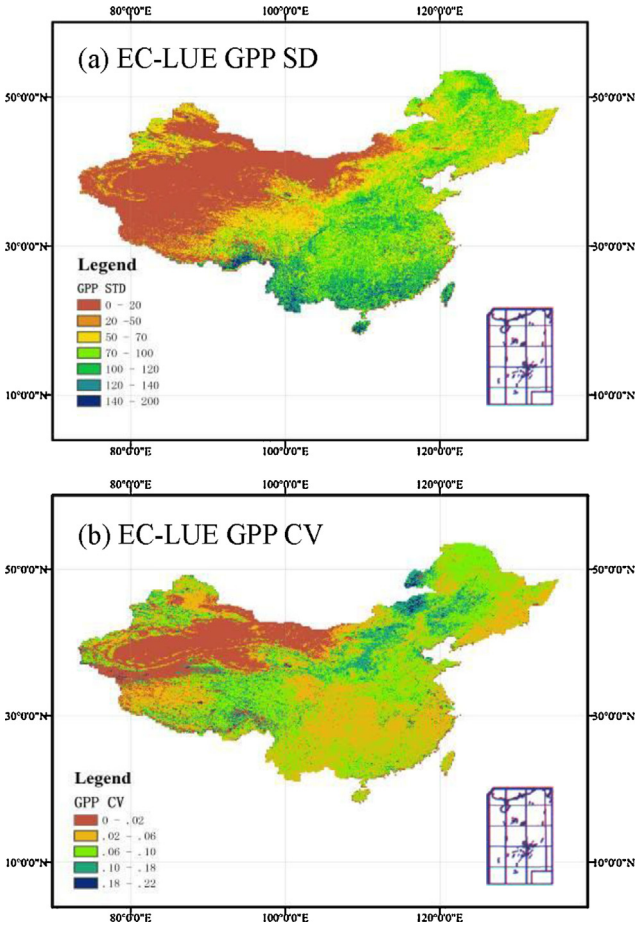

Fig. 10. Spatial distribution of the variability in GPP estimates as represented by (a) the standard deviation (SD, g C m^{-2} yr^{-1}) of model GPP estimates in a grid cell, and (b) the coefficient of variance (CV) of model GPP estimated in a grid cell. The coefficient of variance is determined by dividing the standard deviation by the mean of the model GPP estimates within a grid cell.

The standard deviation and the coefficient of variation were used to indicate absolute inter-annual variability (AIAV) and relative inter-annual variability (RIAV) of the GPP, respectively. Relatively high AIAVs occurred for the evergreen broadleaf forests, permanent wetlands, and evergreen needleleaf forests with a SD of 119 g C m^{-2} yr^{-1}, 81 g C m^{-2} yr^{-1} and 77 g C m^{-2} yr^{-1}, respectively (Table 4). Open shrublands and grasslands showed AIAVs with a STD of 19 g C m^{-2} yr^{-1} and 34 g C m^{-2} yr^{-1}, respectively. Generally, the AIAV of the GPP was large where the GPP was high and small where the GPP was low (Fig. 10a; Table 4). The AIAV of the GPP among various land cover types had significant correlations with the AIAVs in air temperature ($R^2 = 0.66$, $P < 0.05$), precipitation ($R^2 = 0.71$, $P < 0.05$), and NDVI ($R^2 = 0.83$, $P < 0.05$), respectively, across all the biomes, indicating that vegetation index and meteorological parameters are important factors affecting AIVI of GPP in China. The observed inter-annual variability in GPP at the Takayama was also influenced by changes in vegetation characteristics such as leaf area index (Higuchi et al., 2005).

The RIAVs of the GPP were less than 10% for all the biomes (Table 4). There were large RIAVs with a CV of 5.9%, 5.2% and 5.6% in the evergreen broadleaf forests, deciduous broadleaf forest, and mixed forests, respectively. The maximum RIAV occurred for savannas and grasslands with a CV of 9.4% and 8.8%, respectively (Table 4). The trend was similar to the spatial distribution of the variability in GPP estimates as represented by the coefficient variance of model GPP estimated in a grid cell (Fig. 10b). No significant

relationship was found between the RIAV of the annual GPP and the vegetation index and multiple meteorological factors in this study. Fang et al. (2001) used an annual mean NDVI data set over China to quantify temporal net primary production (NPP) variability relative to precipitation variation, finding that the correlation between CVs for NDVI and or NPP and precipitation were identified as statistically significant. Compared with Fang et al. (2001), opposite trend between inter-annual variability in NPP and precipitation was observed by Knapp and Smith (2001) from 11 Long Term Ecological Research sites across North America, aboveground NPP being responded more strongly to wet than to dry years. The inter-annual variability of GPP that resulted from the variation of precipitation and the vegetation index may be due to climate variability and disturbances.

4. Conclusions

Based on EC measurements and remote sensing data, the EC-LUE model was capable of tracking seasonal dynamics and spatial variations in GPP estimation of various vegetation types in China's terrestrial ecosystem and explained about 62–79% of the GPP variations of C_4 and C_3 vegetations, respectively. The annual GPP in China varied between 5.63 Pg C yr^{-1} and 6.39 Pg C yr^{-1} during the period from 2000 to 2009, with a mean value of 6.04 Pg C yr^{-1}, which accounted for 4.90–6.29% of the global GPP. Similar distribution was found between EC-LUE GPP and MODIS product except some provinces such as Xinjiang, Tibet, and Ningxia in the northwestern China. The spatio-temporal distribution of GPP was associated with land cover types and climate zones. Vegetation indexes (e.g., NDVI) and meteorological factors (e.g., air temperature and precipitation) significantly ($R^2 = 0.66–0.83$, $P < 0.05$) affected the absolute inter-annual variability of GPP. Five of the most productive vegetation types including croplands, mixed forests, grasslands, woody savannas, and natural vegetation mosaics, assimilated 81% of the terrestrial carbon in China. Monthly GPP between June and August accounted for 48.8% of the annual vegetation production, whereas that between November and February contributed only 13.1%. In this study, most of the vegetation types showed higher regional GPP densities than global GPP densities by a factor of 1.74–1.98, but a high proportion of sparsely vegetated areas resulted in the low GPP for Chinese terrestrial ecosystems.

Authors' contributions

Liang, S.L. and Yuan, W.P. designed research; Li, X.L., Yu, G.R., Xia, J.Z. and Cheng, X. performed research; Zhao, T.B., Feng, J.M., Ma, Zh.G., Liu, S.M., Chen, J.Q., Shao, C.L., Li, S.G., Zhang, X.D., Zhang, Zh.Q., Chen, S.P., Ohta, T., Varlagin, A., Miyata, A., Takagi, K., Saiqusa, N. and Kato, T. contributed new EC site data/analytic tools; Li, X.L. and Yuan, W.P. analyzed data; Li, X.L. wrote the paper.

Acknowledgements

We acknowledge the financial support from National High Technology Research and Development Program of China (863 Program) (2013AA122003), and National Key Basic Research and Development Plan of China (2011CB952001) and the Fundamental Research Funds for the Central Universities. We also acknowledge the Coordinated Observations and Integrated Research over Arid and Semi-arid China (COIRAS) (lead by Key Laboratory of Regional Climate-Environment Research for the Temperate East Asia (REC-TEA)).

References

Alton, P.B., 2011. How useful are plant functional types in global simulations of the carbon, water, and energy cycles? Journal of Geophysical Research 116, http://dx.doi.org/10.1029/2010JG001430.

Baldocchi, D.D., Valentini, R., Running, S.R., Oechel, W., Dahlman, R., 1996. Strategies for measuring and modelling CO_2 and water vapor fluxes over terrestrial ecosystems. Global Change Biology 2, 159–168.

Beer, C., Reichstein, M., Tomelleri, E., Ciais, P., Jung, M., Carvalhais, N., Rödenbeck, C., et al., 2010. Terrestrial gross carbon dioxide uptake: global distribution and covariation with climate. Science 329, 834–838, http://dx.doi.org/10.1126/science.1184984.

Canadell, J.G., Mooney, H.A., Baldocchi, D.D., Berry, J.A., Ehleringer, B., Field, C.B., Gower, S.T., et al., 2000. Carbon metabolism of the terrestrial biosphere: a multi-technique approach for improved understanding. Ecosystems 3, 115–130.

Canadell, J.G., Pataki, D., Gifford, R., Houghton, R., Luo, Y., Raupach, M., et al., 2007. Saturation of the terrestrial carbon sink. In: Canadell, J.G., Pataki, D., Pitelka, L. (Eds.), Terrestrial Ecosystems in a Changing World IGBP Series. Springer, Berlin, pp. 81–100.

Cao, M.C., Fian, W., 1998. Net primary and ecosystem production and carbon stocks of terrestrial ecosystems and their responses to climate change. Global Change Biology 4, 185–198.

Chapin, M.C., Matson, P.A., Mooney, H.A. (Eds.), 2002. Principles of Terrestrial Ecosystem Ecology. Springer-Verlag, New York, Berlin, Heidelberg, p. 102.

Chen, L.J., Liu, G.H., Feng, X.F., 2001. Estimation of net primary productivity of terrestrial vegetation in China by remote sensing. Acta Botania Sinica 43 (11), 1191–1198.

Chen, J.M., Chen, B.Z., Higuchi, K., Liu, J., Chan, D., Worthy, D., 2006. Boreal ecosystems sequestered more carbon in warmer year. Geophysical Research Letters 33, L10803, http://dx.doi.org/10.1029/2006GL025919.

Desai, A.R., Richardson, A.D., Moffat, A.M., Kattge, J., Hollinger, D.Y., Barr, A., Falge, E., Noormets, A., Papale, D., Reichstein, M., Stauch, V.J., 2008. Cross site evaluation of eddy covariance GPP and RE decomposition techniques. Agricultural and Forest Meteorology 148 (6–7), 821–838, http://dx.doi.org/10.1016/j.agrformet.2007.11.012.

Fang, J.Y., Yoda, K., 1990. Vegetation and climate in China. III. Water balance in relation to distribution of vegetation. Ecological Research 4, 71–83.

Fang, J.Y., Piao, S.L., Tang, Z.Y., Peng, C.H., Ji, W., 2001. Interannual variability in net primary production and precipitation. Science 293, 1723a.

FAOSTAT, 2008. Harvested area of Maize in China during the period of 2008. http://faostat.fao.org/site/567/DesktopDefault.aspx?PageID=567#ancor

Feng, X., Liu, G., Chen, J.M., Chen, M., Liu, J., Ju, W., Sun, R., Zhou, W., 2007. Simulating net primary productivity of terrestrial ecosystems in China using a process model driven by remote sensing. Journal of Environmental Management 85, 563–573.

Friend, A.D., Arneth, A., Kiang, N.Y., Lomas, M., Ogee, J., Rodenbeck, C., et al., 2007. FLUXNET and modelling the global carbon cycle. Global Change Biology 13, 610–633.

Global Modeling and Assimilation Office, 2004. File Specification for GEOSDAS Gridded Output Version 5.3, Report. NASA Goddard Space Flight Cent, Greenbelt, MD.

Gong, P., Xu, M., Chen, J., 2002. A preliminary study on the carbon dynamics of China's terrestrial ecosystems in the past 20 years. Earth Science Frontiers 9 (1), 55–61.

Higuchi, K., Shashkov, A., Chan, D., Saigusa, N., Murayama, S., Yamamoto, S., Kondo, H., Chen, J., Liu, J., Chen, B., 2005. Simulations of seasonal and intra-annual variability of gross primary productivity at Takayama with BEPS ecosystem model. Agriculture and Forest Meteorology 134, 143–150.

Hwang, T., Kang, S., Kim, J., Kim, Y., Lee, D., Band, L., 2008. Evaluating drought effect on MODIS Gross Primary Production (GPP) with an eco-hydrological model in the mountainous forest, East Asia. Global Change Biology 14, 1–20, http://dx.doi.org/10.1111/j.1365-2486.2008.01556.x.

Knapp, A.K., Smith, M.D., 2001. Variation among biomes in temporal dynamics of aboveground primary production. Science 291, 481.

Landsberg, J.J., Waring, R.H., 1997. A generalised model of forest productivity using simplified concepts of radiation-use efficiency, carbon balance and partitioning. Forest Ecology and Management 95, 209–228.

Liu, M.L., 2001. Land use/cover change and terrestrial ecosystem phytomass carbon pool and production in China. In: The Doctoral Dissertation of the Institute of Remote Sensing Application, CAS (in Chinese with English abstract).

Liu, J., Chen, J.M., Cihlar, J., Chen, W., 1999. Net primary productivity distribution in the BOREAS region from a process model using satellite and surface data. Journal of Geophysics Research 104 (D22), http://dx.doi.org/10.1029/1999JD900768, 27, 735–754.

Mu, Q.Z., Zhao, M.S., Heinsch, F.A., Liu, M.L., Tian, H.Q., Running, S.W., 2007. Evaluating water stress controls on primary production in biogeochemical and remote sensing based models. Journal of Geophysical Research-Biogeosciences 112, G01012.

Piao, S.L., Fang, J.Y., Guo, Q.H., 2001. Application of CASA model to the estimation of Chinese terrestrial net primary production. Acta Phytoecologica Sinca 25 (5), 603–608 (in Chinese with English abstract).

Potter, C.S., Randerson, J.T., Field, C.B., Matson, P.A., Mooney, H.A., Klooster, S.A., 1993. Terrestrial ecosystem production: a process model based on global satellite and surface data. Global Biogeochemical Cycle 7, 811–841.

Running, S.W., Nemani, R., Glassy, J.M., Thornton, P.E., 1999. MODIS daily photosynthesis (PSN) and annual net primary production (NPP) product (MOD17), algorithm theoretical basis document, version 3.0. In: http://modis.gsfc.nasa.gov/

Running, S.W., Thornton, P.E., Nemani, R., Glassy, J.M., 2000. Global terrestrial gross and net primary productivity from the earth observing system. In: Sala, O.E., Jackson, R.B., Mooney, H.A. (Eds.), Methods in Ecosystem Science. Springer Verlag, New York, pp. 44–57.

Running, S.W., Nemani, R.R., Heinsch, F.A., Zhao, M.S., Reeves, M., Hashimoto, H., 2004. A continuous satellite-derived measure of global terrestrial primary production. Bioscience 54, 547–560.

Saigusa, N., Yamamoto, S., Murayama, S., Kondo, H., 2005. Inter-annual variability of carbon budget components in an AsiaFlux forest site estimated by long-term flux measurements. Agricultural and Forest Meteorology 134, 4–16.

Suyker, A.E., Verma, S.B., Burba, G.G., Arkebauer, T.J., 2005. Gross primary production and ecosystem respiration of irrigated maize and irrigated soybean during a growing season. Agricultural and Forest Meteorology 131, 180–190.

Tao, B., Li, K., Shao, X.M., Cao, M.K., 2003. The temporary and spatial patterns of terrestrial net primary productivity in China. Journal of Geographical Sciences 13 (2), 163–171.

Turner, D.P., Urbanski, S., Bremer, D., Wofsy, S.C., Meyers, T., Gower, S.T., et al., 2003. A cross-biome comparison of daily light use efficiency for gross primary production. Global Change Biology 9, 383–395.

Verbeeck, H., Samson, R., Verdonck, F., Lemeur, R., 2006. Parameter sensitivity and uncertainty of the forest carbon flux model FORUG: a Monte Carlo analysis. Tree Physiology 26, 807–817.

Xiao, X., Melillo, J.M., Kicklighter, D.W., Pan, Y., McGuire, A.D., Helfrich, J., 1998. Net primary production of terrestrial ecosystems in China and its equilibrium responses to changes in climate and atmospheric CO_2 concentration. Acta Phytoecologica Sinca 22, 97–118.

Xiao, X.M., Hollinger, D., Aber, J., Goltz, M., Davidson, E.A., Zhang, Q.Y., Moore III, B., 2004. Satellite-based modeling of gross primary production in an evergreen needleleaf forest. Remote Sensing of Environment 89, 519–534.

Xiao, J.F., Zhuang, Q.L., Law, B.E., Chen, J.Q., Baldocchi, D.D., Cook, D.R., et al., 2010. A continuous measure of gross primary production for the conterminous United States derived from MODIS and AmeriFlux data. Remote Sensing of Environment 114, 576–591.

Yuan, W.P., Liu, S.G., Zhou, G.S., Zhou, G.Y., Tieszen, L.L., Baldocchi, D., et al., 2007. Deriving a light use efficiency model from eddy covariance flux data for predicting daily gross primary production across biomes. Agricultural and Forest Meteorology 143, 189–207.

Yuan, W.P., Liu, S.G., Yu, G.R., Bonnefond, J.M., Chen, J.Q., Davis, K., et al., 2010. Global estimates of evapotranspiration and gross primary production based on MODIS and global meteorology data. Remote Sensing of Environment 114, 1416–1431.

Zhang, Y., Yu, Q., Jiang, J., Tang, Y., 2008. Calibration of Terra/MODIS gross primary production over an irrigated cropland on the North China Plain and an alpine meadow on the Tibetan Plateau. Global Change Biology 14, 757–767.

Zhao, M., Running, S.W., 2010. Drought-induced reduction in global terrestrial net primary production from 2000 through 2009. Science 329, 940–943.

Zhao, M., Heinsch, F.A., Nemani, R., Running, S.W., 2005. Improvements of the MODIS terrestrial gross and net primary production global data set. Remote Sensing of Environment 95, 164–176.

Zhao, M., Running, S.W., Nemani, R.R., 2006. Sensitivity of Moderate Resolution Imaging Spectroradiometer (MODIS) terrestrial primary production to the accuracy of meteorological reanalyses. Journal of Geophysical Research 111, G01002, http://dx.doi.org/10.1029/2004JG000004.

Zhu, W.Q., Pan, Y.Z., Zhang, J.S., 2007. Estimation of net primary productivity of Chinese terrestrial vegetation based on remote sensing. Journal of Plant Ecology 31, 413–424.